A Combined Theoretical and Experimental Study of Small Anthracene-Water Clusters

Estefania Rossich Molina,[a] Bo Xu,[b] Oleg Kostko,[b] Musahid Ahmed,*[b]

Tamar Stein*[a]

[a] *Fritz Haber Research Center for Molecular Dynamics, Hebrew University of Jerusalem, Jerusalem 9190401, Israel*

[b] *Chemical Sciences Division, Lawrence Berkeley National Laboratory, Berkeley, California 94720,* USA

Abstract

Water-cluster interactions with polycyclic aromatic hydrocarbons (PAHs) are of paramount interest in many chemical and biological processes. We report a study of anthracene monomers and dimers with water (up to four)-cluster systems utilizing molecular beam vacuum-UV photoionization mass spectrometry and density functional calculations. Structural loss in photoionization efficiency curves when adding water indicates that various isomers are generated, while theory indicates only a slight shift in energy in photoionization states of different isomers. Calculations reveal that the energetic tendency of water is to remain clustered and not to disperse around the PAH. Theoretically, we observe water confinement exclusively in the case of four water clusters and only when the anthracenes are in a cross configuration due to optimal OH$\cdots\pi$ interactions, indicating dependence on the size and structure of the PAH. Furthermore theory sheds light on the structural changes that occur in water upon ionization of anthracene, due to the optimal interactions of the resulting hole and water hydrogen atoms.

Introduction

The non-covalent interactions of polyaromatic hydrocarbons (PAHs) with water have drawn much attention due to their importance in chemical, environmental, astrochemical, and biological processes.[1] Small PAHs can act as a model for understanding water graphite and graphene interactions,[2] driven by the large societal interest in water purification and hydrogen production in the confinement of carbon nanotubes.[3] This is due to the nature of water interactions in nanometer-scale pores and capillaries. There have been suggestions that water takes on an increased structural order in nanoconfined geometries, resulting in a technological application of acene-type molecules;[4] embedding them within synthetic nanostructures allows for fast transport of water through membranes.[5, 6] There is also interest in how aromatic systems with π clouds[7] can be used for molecular recognition[8], relevant in both sensing and medical applications. In cold interstellar regions, PAHs can freeze on icy mantles formed on dust grains,[9] where UV and VUV processing can occur on these ices. The subsequent photochemistry can be ion- or radical-mediated, giving rise to possibly complex new molecules due to dehydrogenation, charge or proton transfer that occur after the initial ionization event.[10] There is much discussion on how PAHs embedded in water ice can lead to a lowering of ionization energies during UV processing.[11]

In recent years, increasingly sophisticated experimental and theoretical tools have been brought to bear on understanding PAH and water-cluster interactions. Rotational and IR spectroscopy on a series of PAHs solvated by water clusters showed subtle non-covalent intermolecular interactions.[12-15] Ion mobility coupled with density functional theory (DFT) was used to study naphthalene water and methanol-cluster thermodynamics.[16] It was postulated that in the case of water, there is external solvation, and upon clustering, chains mediated by CH···O interactions are formed. Vibrational and electronic spectroscopy revealed that in protonated naphthalene-water monomers, the proton is located on the naphthalene, and that the process is dramatically reversed with the addition of a second water molecule.[17] In related work, the electronic spectroscopy of anthracene-water clusters was mapped out almost three decades ago with resonant photoionization.[18] Using ion thermochemistry, it was shown[19] that there was no reaction between the naphthalene cation and water. However, the reaction with the naphthyl radical was facile. Infrared spectroscopic studies[20] of naphthalene-water monomers and dimers have been extended to larger water clusters of up to five molecules that reveal the differences between benzene and the effects of adding a ring to solvation.[21] Anion two-dimensional photoelectron spectroscopy revealed that incremental solvation of anionic anthracene by up to five water molecules led to enhanced formation mediated by a bound excited state of the anion.[22]

Due to the great importance of a molecular-level understanding of PAH-water interactions, many theoretical studies have focused on important bonding patterns governing these interactions. The electronically excited states, binding energies (BE) and hydrogen-bonding interactions have been studied using wave-function and DFT methods on the naphthalene-water-hexamer system. The interaction of the water cluster with the aromatic rings is via OH$\cdots\pi$ and CH$\cdots$O type interactions. OH$\cdots\pi$ interactions were found to dominate, and the $\pi-\pi^*$ transition in naphthalene was redshifted upon solvation by the water cluster. An empirical potential was used to model the interactions of 20 water clusters around C_{60}, coronene and corannulene cations.[23] The salient finding was that a water cluster was formed next to the ion and that the $(H_2O)_4X^+$ species, where X is the relevant PAH, was often the most stable. An analysis of the binding energies and dynamics indicated that water-water interactions dominated over the water-seed interactions, suggesting that water does not wet the hydrocarbon. Hirunsit and Balbuena[24] used benzene and naphthalene complexed with water clusters (1-4) to study the optimal interactions. They claimed that water tends to maximize the number of hydrogen bonds above the surface and forms a cyclic network. A recent high-level theoretical calculation of the water dimer on naphthalene confirmed the suggestion that OH$\cdots$O interactions dominate, leading to a dimer sitting on the surface, with the hydrogen in the water molecules interacting with the π cloud and one of the oxygen atoms interacting with the hydrogen atoms in the naphthalene.[25] Hirunsit and Balbuena[24] also probed the effects of confinement of water clusters on the properties of water and proton transfer. Interestingly, confining the water cluster between two naphthalene molecules was only obtained by imposing constraints on the systems. Lifting the constraints resulted in a rearrangement of the confined structure to a non-confined structure. Directly relevant to the present study are a series of theoretical papers that discuss the energetics and structures of PAH clusters,[26] particularly the dimerization of anthracene.[27, 28]

In a recently published study of naphthalene-water clusters using a combined experimental and theoretical approach, we demonstrated that different channels of ionization of the naphthalene-water clusters depended on the energy of the ionizing photon. When the photon energy was below the water-ionization value threshold, the naphthalene moiety of the cluster was ionized, and no protonated, naphthalene-water clusters were observed.[29] The study showed that rearrangements of the water sub-cluster upon ionization enhance their charge dipole interactions and other induced interactions with cationic naphthalene while maintaining the hydrogen-bonding network. There is proton transfer within the water-sub-cluster and hydroxyl radical emission when ionization occurs above the water ionization threshold. In addition, the generated hydroxyl radical can also react with naphthalene to form an adduct, and the remaining water molecules solvate the protons.

Here, we study the structural motifs and photoionization dynamics of anthracene-water clusters with synchrotron-based VUV photoionization mass spectrometry measurements coupled to a supersonic molecular beam expansion. The experimental results are coupled with electronic structure calculations to elucidate the

effect of water on the photoionization dynamics of anthracene and its dimer. We analyze the possible isomers formed in the molecular beam (before and after ionization) containing monomer and dimer anthracene with up to four water molecules. Additionally, we study different possible isomers corresponding to the different orientations of the water clusters with respect to the anthracene monomers and dimers. The photoionization efficiency (PIE) curve suggests that various isomers are formed in the experiment. Our results demonstrate that the energetic tendency of the water clusters is to remain clustered together. In addition to the hydrogen bonds between the water molecules, hydrogen bonds also form with the aromatic ring, which dictates the stability of the different isomers. Ionization of the anthracene leads to structural changes in the water clusters. Theoretically we show that water confinement inside two anthracenes is not energetically preferred in the case of one to three water molecules, similar to previous results on water confinement within two naphthalene units. However, unlike the naphthalene case, four water clusters can be confined between two anthracenes when they are in cross configuration due to an additional stabilizing OH$\cdots\pi$ interaction.

Experimental Section

The experiments were performed with a reflectron time-of-flight mass spectrometer incorporating a continuous supersonic expansion molecular beam source. The apparatus is coupled to a 3-meter vacuum monochromator on the Chemical Dynamics Beamline (9.0.2) located at the Advanced Light Source and has been described in our previous studies.[29] Anthracene was placed at the front end of a stainless-steel nozzle, which has a 50 µm diameter center hole and was heated to 381 K using a cartridge heater. Anthracene vapor was diffused into 820 Torr argon carrier gas seeded with water vapor. The gas mixture passed through the 50 µm hole and expanded supersonically in a vacuum to produce a molecular beam in the interaction region of a reflectron time-of-flight mass spectrometer, where the neutral clusters were ionized by the VUV light and subsequently detected. Mass spectra were recorded in a photon energy range between 7 and 12.5 eV in a photon energy step size of 50 meV. The PIE curves of the water clusters were obtained by integrating over the peaks in the mass spectrum at each photon energy and were normalized by the photon flux.

Computational Methods

All calculations in this manuscript were performed using Q-Chem software.[30] Optimal structures were obtained using the wB97X-V functional.[31] Optimization calculations on the monomer were performed using the aug-cc-pVTZ basis set. For all dimer calculations, we used the cc-pVDZ basis set.[32] Frequency calculations followed optimization of the structures to verify that they were indeed minima on the potential energy surface (PES). Single-point calculations using the aug-cc-pVTZ basis set were performed on all the optimized dimer structures to obtain the binding energies (BE). To model the experimental results, we started by building neutral clusters

containing anthracene monomers and dimers with water clusters of one to four molecules, as observed experimentally. The neutral clusters were then optimized on the cationic surface to account for the structural changes upon ionization. The ionized states were calculated using the ionization-potential variant of the equation of motion coupled cluster with single and double corrections (EOM-IP-CCSD) using the cc-pVDZ basis set.[33-35] Calculations employed the RI approximation for the treatment of the two-electron integrals.[36] EOM-CCSD includes dynamic and non-dynamic correlation effects and provides accurate ionization and excitation energies.

Results and Discussion

Experimental Mass Spectra

The photoionization mass spectra of the anthracene water clusters recorded at 10 eV photon energy is shown in figure 1A for argon backing pressure of 820 torr and the heater temperature to sublimate anthracene in the nozzle maintained at 381 K. The strongest signal arises from the anthracene monomer (178 amu), followed by a series of peaks in an increment of 18 amu (water monomer) up to n=9, where n is the number of water molecules attached to anthracene. The dimer of anthracene is recorded at 356 amu, and in this case water attachment up to n= 4 to the dimer can be detected in the mass spectrum. Peaks are also recorded for anthracene clustered with one, two, or three argon atoms, as marked in the figure. The source conditions (backing pressure, nozzle diameter & nozzle temperature) were varied to optimize conditions so that reasonable amounts of anthracene monomers and dimers and their clusters could be formed. Previously we have demonstrated that smaller nozzle sizes and larger backing pressures could give rise to formation of large argon clusters which could skew the dynamics of cluster formation. [37, 38]. The inset of figure 1A shows an expanded region of the mass spectrum between 213 and 220 m/z. The main peaks are for anthracene clustered with two waters and one argon respectively, while the smaller peaks separated by 1 amu arise from the ^{13}C natural isotope contribution. At this photon energy, there is no evidence of protonated species being present in the clusters that are formed in the molecular beam.

However, upon increasing the photon energy beyond 11 eV, when water clusters begin to ionize, there is proton transfer and the formation of pure protonated water clusters in the molecular beam. This is evidenced in figure 1B, for photoionization at 12.5 eV, where in addition of the monomer anthracene peak, a series of water clusters can be discerned up to n= 19. The series of peaks originating at m/z 43 and extends up to m/z 385 with a spacing of m/z 18 originated from metastable decay of anthracene water cluster ions. The inset which expands m/z 53-57, shows the spectra in green for the protonated water trimer $H^+(H_2O)_3$ at m/z 55 and no evidence for the non-protonated trimer at m/z 54. Also shown is the expanded mass spectra in red for anthracene with two water molecules (214 amu), and m/z 215. At this particular photon energy of 12.5 eV, there is some contribution to m/z 215 from proton transfer from water to anthracene similar to what was observed for naphthalene water clusters.[29] This occurs due to ionization of water, as is shown by tracking its appearance

energy as shown in the supplementary information. Plotting the ratios of intensities between the species and +1 m/z provides an easy way to separate out the contribution of ^{13}C from H^+. The figure shows only contribution of ^{13}C (0.15%) till around 11.2 eV, and then begins to rise due to ionization of the 3A"orbital of water.[35] The rate of proton transfer to anthracene from water is much less than that observed for naphthalene water suggesting that ring size could play a role in the transfer dynamics.

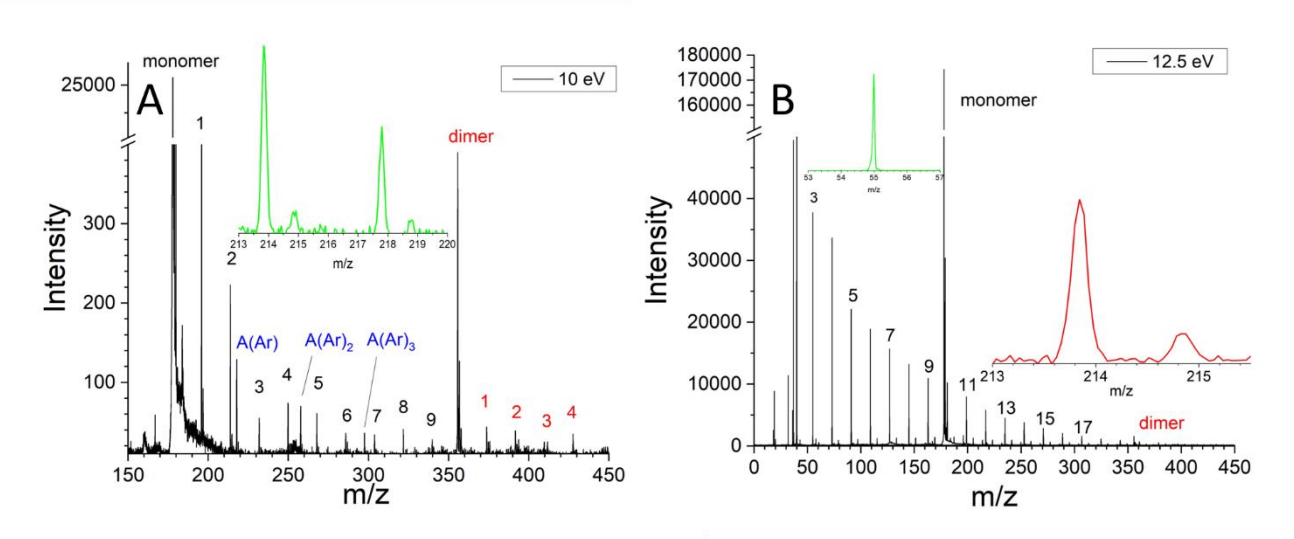

Figure 1: Mass spectra of anthracene-water clusters recorded at (A) 10 eV and (B) 12.5 eV photon energy, with an Ar-backing pressure of 820 Torr, and heater temperature of 381 K. The green inset in (A) shows an expanded range of the mass spec between 213-220 m/z, while the green inset in (B) shows the range between 53-57 m/z, and the red inset shows the range between 213-215.5 m/z. The series of peaks originating at m/z 43 and extends up to m/z 385 with a spacing of m/z 18 originated from metastable decay of anthracene water cluster ions.

To computationally model the experimental results, we start by studying the structures of neutral clusters containing anthracene and water formed prior to photoionization. We then re-optimize the structures on the cationic surface to model structural changes following ionization. To study the mutual effect of the aromatic ring and the water cluster, we focus on water clusters containing one to four water molecules complexed with the anthracene monomer and dimer.

Neutral Anthracene-Water Cluster

It was previously demonstrated that the naphthalene water sub-clusters could be in different orientations with respect to the aromatic ring; specifically, two orientations were reported, an "on-top" orientation and a "side" orientation, with a general preference for the "on-top" orientation (only with two water molecules is the side orientation more stable).[29]

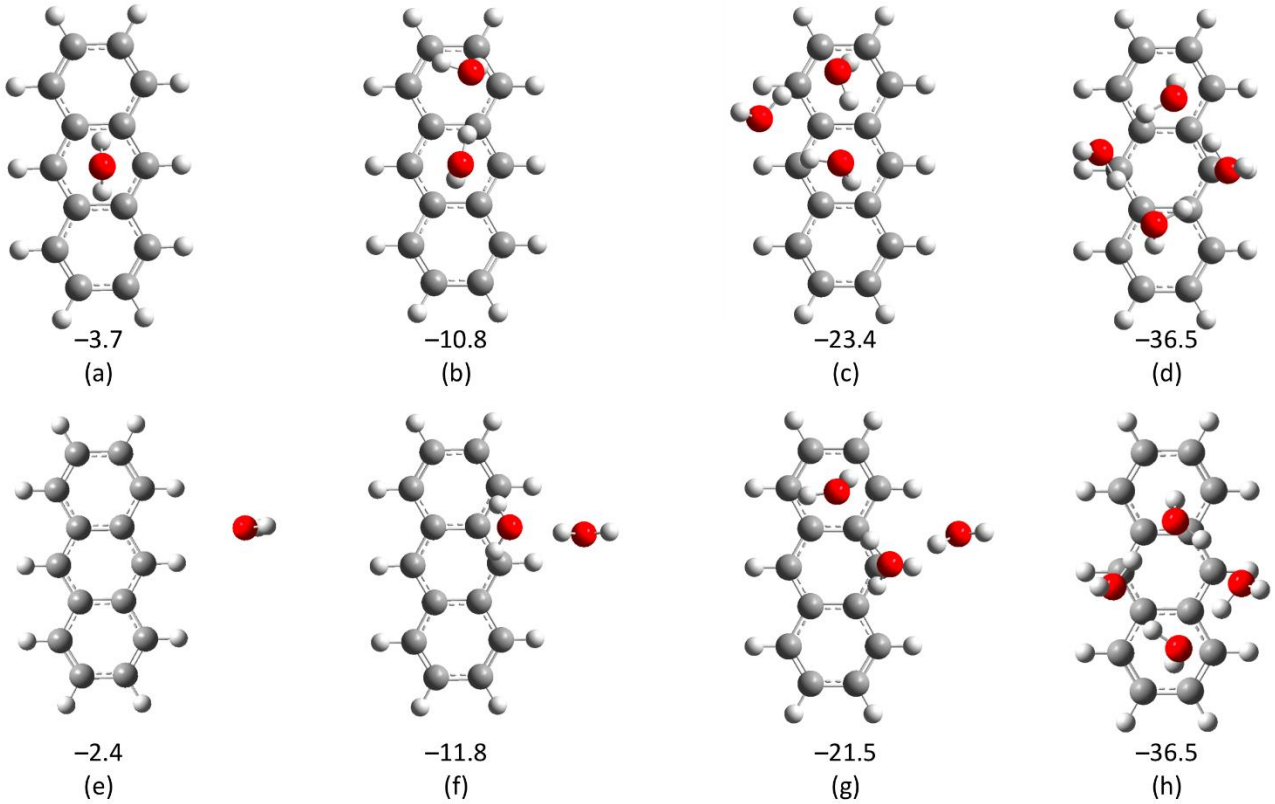

Figure 2 Top: Anthracene with water sub-cluster in the "on-top" orientation. Bottom: Anthracene with water sub-cluster in the "side" orientation. BEs are given in kcal/mol.

Figure 2 presents anthracene-water clusters in the two discussed orientations. Here, we observe that the preference of the water cluster is to form sub-clusters similar to those found in isolated water clusters[39, 40] on top of the anthracene ring. This orientation is more stable in all cases except in the case of two water molecules where the "side" orientation is more stable, similar to the trends reported for the naphthalene case.[29] In the case of four water molecules, the two initial structures ("side" and "on-top") converged to the same minima, where the water forms an optimal sub-cluster on top of the aromatic ring.

The structures of the anthracene dimer were calculated to explore possible orientations of the water sub-clusters on it. Results of different isomers of the anthracene dimer are presented in Figure 3. For each isomer, we report the BE, which is calculated according to $BE = E_{dimer} - 2 \times E_{anthracene}$.

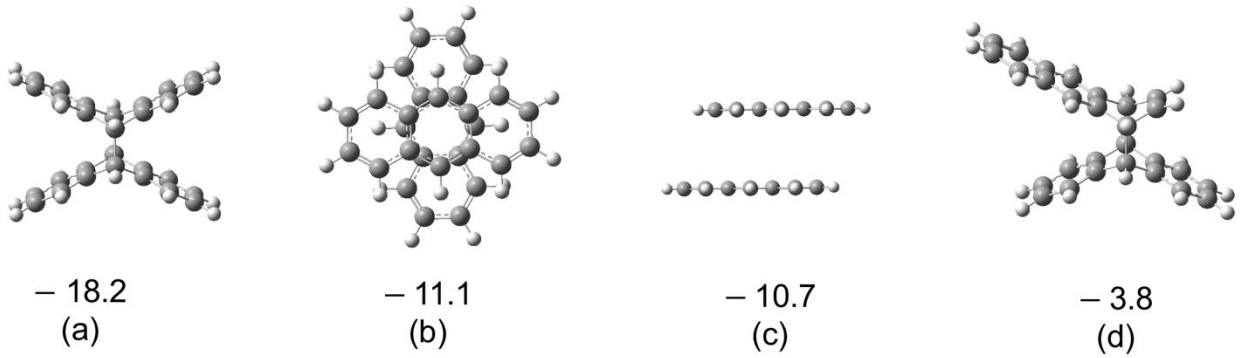

Figure 3: Structure of neutral anthracene dimers. Structure (a) is a bonded structure in which a bond is formed via a bridge between the central rings, and Structure (d) is a bonded structure where the bond is formed via a terminal ring of one anthracene and the central ring of the second anthracene. Structures (b) and (c) are stacked configurations with different orientations of the anthracene units.

The most stable dimer structure is (a), where the two units of anthracene are bonded via a bridge between the central rings, with a BE of -18.2 kcal/mol. Structures (b) and (c) are stacked configurations with a slight difference of 0.4 kcal/mol in their BEs. Structure (d) is also a bridge structure, albeit here, the bridge is formed between the central ring of one unit and a terminal ring of the second unit. In this case, the isomer is the least stable and has the lowest BE of the studied isomers.
Structure (a) is the result of [4+4]-cycloaddition on anthracene which can form upon exposure to radiation and is thus highly unlikely to form under the neutral expansion conditions of our experiment.
We now turn to calculate structures of the anthracene dimer with water clusters, W_n, (n=1-4) as observed in the experiment. For completeness, anthracene bonded structure (Fig3(a)) complexed to waters are presented in the SI. When interacting with the dimer, the water cluster can hinder the interaction between the two anthracene molecules resulting in the following configurations:

- All water molecules located between the two anthracene molecules (A-W-A)
- Interspersed configuration, where the anthracene and water molecules are in layers (W-A-W-A)

Alternatively, the anthracene dimers can remain intact. Two kinds of configurations are possible in this case:

- All water molecules are on top of the anthracene dimer (W-A-A)
- The water molecules are divided such that part of the water molecules are on top of the dimer, and the rest are below it (W-A-A-W)

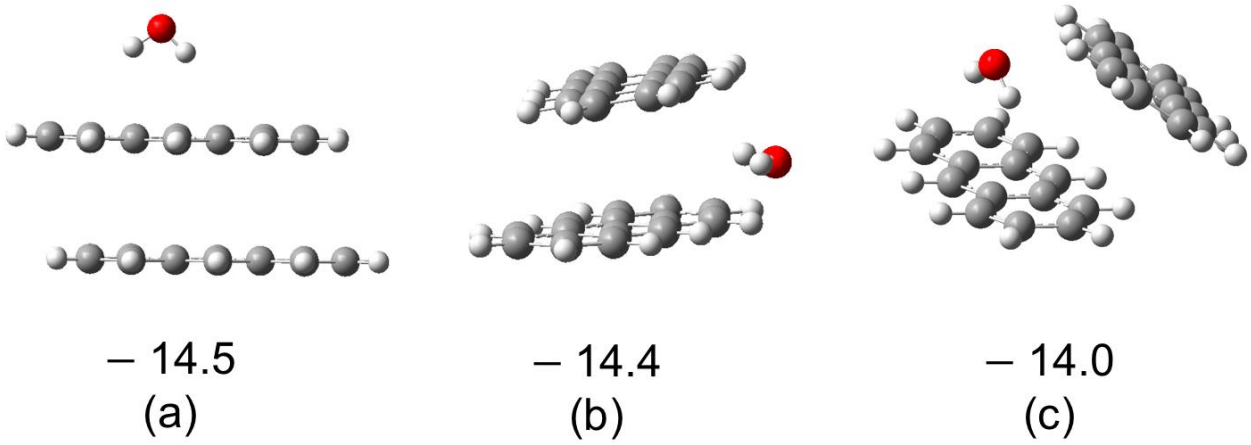

Figure 4: Structures and BEs of two anthracene plus one water molecule complexes. All energies are given in kcal/mol.

Figure 4, presents the results for a neutral complex of two anthracene molecules with one water molecule, and their BEs are calculated via: $E_{BE} = E_{complex} - E_{water} - 2 \times E_{anthracene}$. The considerable stability follows the trend of the isolated dimer, with the bonded structure being the most stable, the bonded structures are presented in Figure S3. All the structures are close in energy. In structure (b), the calculation starts in an orientation in which the water molecule lies between the two anthracenes in the dimer structure; however, we observe that this situation is not favorable, and during optimization, the water molecule does not remain within the anthracenes and moves to the side. The hydrogen atoms in the water molecule point into the dimer, and the distances between the oxygen atom in the water molecule and the four closest hydrogen atoms in the anthracene are between 2.5Å and 3.0Å. In structure (c), the starting point of the calculation had the water molecule inside the dimer structure, and again we observe a movement in the structure so that the water molecule is not confined. The hydrogen atoms in the water molecule point toward the π electrons in the bottom anthracene, and the distance between the two closest hydrogen atoms in the top anthracene and the oxygen atom in the water is 2.5Å and 2.4Å.

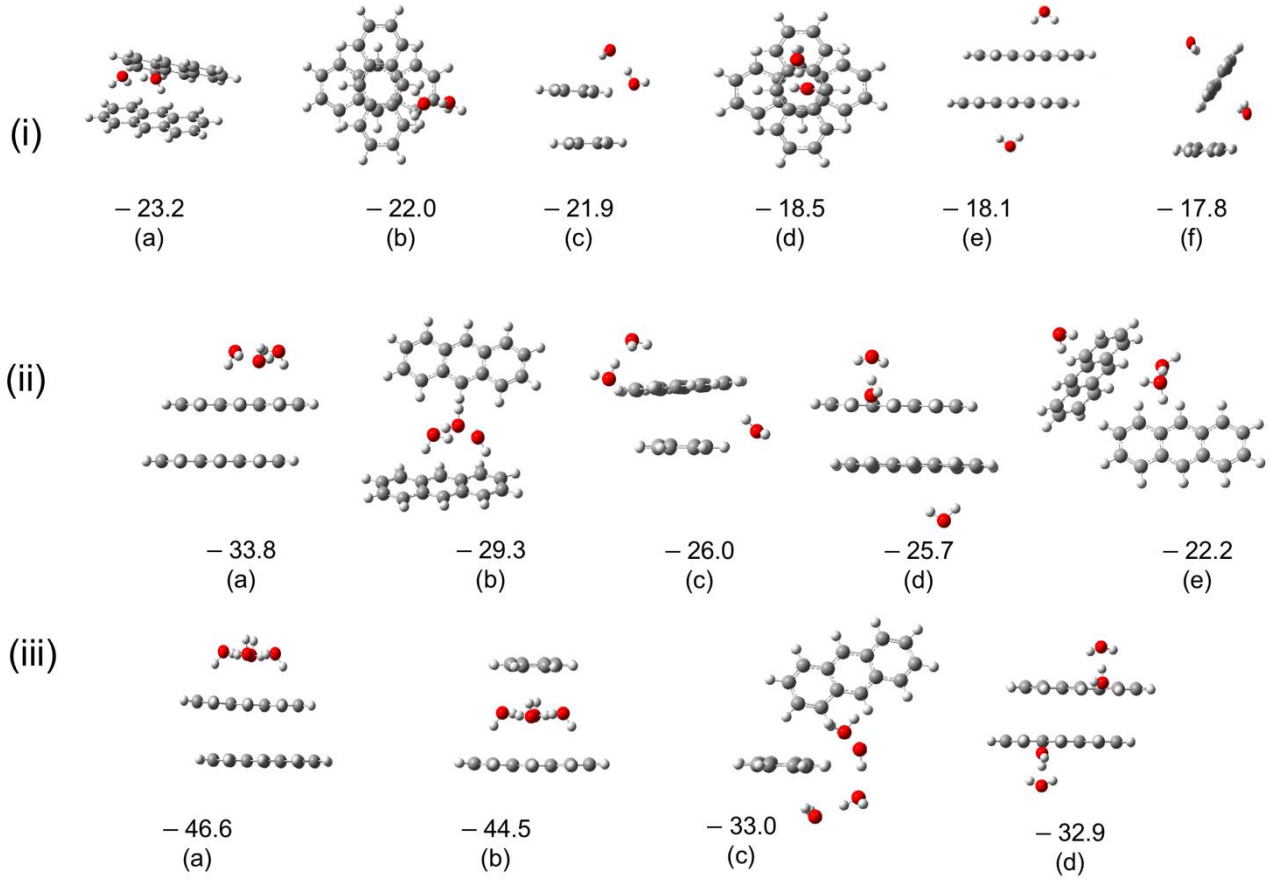

Figure 5: Panel (i): anthracene dimer cluster with two water molecules, Panel (ii): anthracene dimer cluster with three water molecules, and Panel (iii): anthracene dimer cluster with four water molecules. BEs are in kcal/mol.

Similar trends can be observed in the case of the two, three and four water sub-clusters. The stability trends follow those observed for the isolated anthracene dimers; bonded structures are more stable than the non-bonded structures. Bonded structures are presented in Figure S3. The corresponding non-bonded structures and their BEs are presented in Figure 5. In all cases, the structures with the largest BE correspond to the bonded anthracene dimer complexed with water sub-clusters on top of them. The following stable structure is again bonded anthracene, but with the water cluster divided below and on top of the dimers. This trend in the BEs reveals the tendency of the water clusters to remain clustered together and is consistent with the cases of three and four water molecules. These results indicate that the water molecules tend to cluster and not solvate the PAHs. In all cases, the next most stable structure is the non-bonded anthracene dimer in which the water molecules remain clustered to one another. For the two water cases (Figure 5, Panel (i)), structure (i-a) is the next most stable structure. As observed in the case of one water molecule, the water sub-cluster (which starts between the anthracene units) moves to the side so that both anthracenes interact with each other and with the water sub-cluster. Next are structures (i-b) and (i-c), which are very close in energy. In these structures, the water sub-cluster mainly interacts with one of the anthracene units, which leads to a decrease in BE. The least stable

structures, (i-e) and (i-f), has divided water sub-clusters. Similar trends are seen in the case of three and four water molecules in the sub-cluster.

Ionized Clusters

We next turn to a study of photoionized anthracene-water clusters since these are the ones observed in the experiments. Figure 6 presents the structures of one anthracene complexed with a different number of water clusters. As in the neutral case, two possible orientations are possible. In the top orientation, the water molecules remain as a cluster on top of the anthracenes, as shown in Figure 6(i). As the system is now charged (specifically, the anthracene bears a +1 charge), the water rotates so that the oxygen atoms point toward the anthracene. In addition, we observe structures in which the water clusters are on the side of the anthracene and form a chain of hydrogen bonds wherein one oxygen in the water molecules forms a hydrogen bond with the hydrogen atoms in the anthracene, and then forms a chain of water molecules as shown in Figure 6(ii). In the case of four water molecules, the system starting from a side-chain orientation converges to a cyclic water cluster on the side of the anthracene. Figure 6 shows that the side orientation is more stable than the top orientation in the cases of one and two water molecules, while in the cases of three and four molecules, the top orientation is the most stable, which is consistent with a previous study performed on naphthalene.[29]

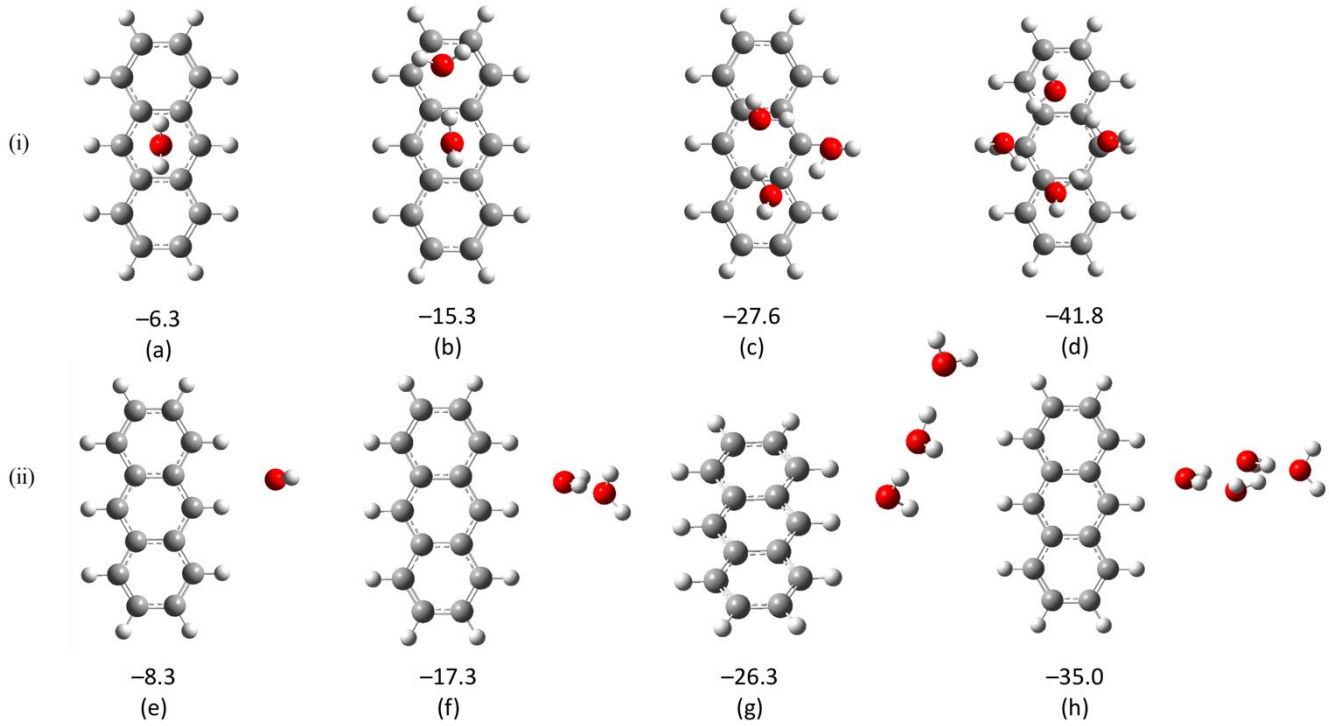

Figure 6: Anthracene dimer complexed to water clusters of various sizes. Top panel: “on-top” orientation. Bottom panel: “side” orientation. BEs are given in kcal/mol.

To study the effect of ionization on the structure of the anthracene dimer water system (A_2W_n), we first studied ionized anthracene dimers separately, as we observed that for the neutral cluster, trends in the stability of the anthracene dimers are preserved when water clusters are present. Re-optimization of the neutral dimers on the cationic surface leads to the structures shown in Figure 7.

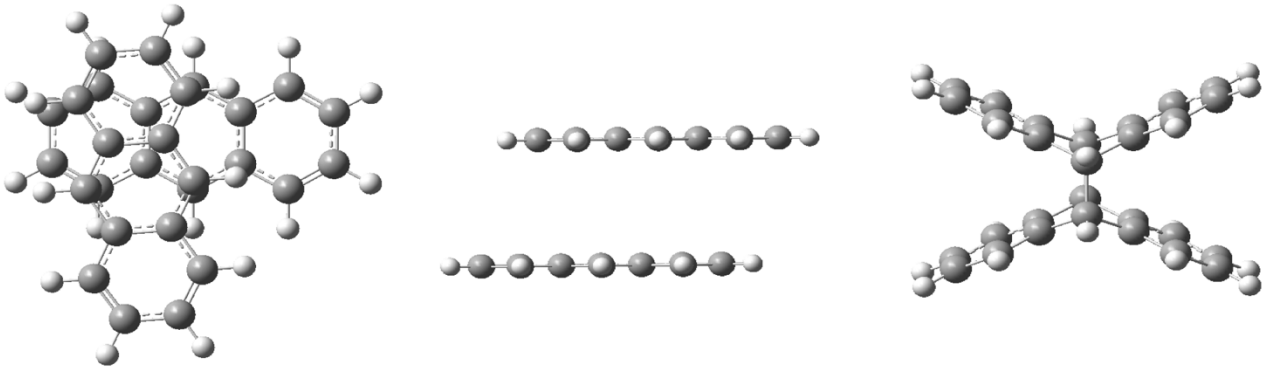

Figure 7: Optimized charged anthracene dimers. BEs are given in kcal/mol.

Interestingly, upon ionization, the trends in the dimer are reversed, and the energetic preference in the cationic dimer is not to be covalently bonded; in fact, the BE of the covalently bonded structure, (c), is approximately 12 kcal/mol less than the other two structures. Thus, we expect the most stable anthracene-water complexes to be with water complexed to structures (a) and (b).

Figure 8 shows ionized anthracene-water complexes. In Figure 8(i), anthracene dimers are complexed to a single water molecule. As expected, the most stable structures are of water complexed to the non-bonded structure, where the side orientation of the water with respect to the anthracene is preferred, in agreement with the ionized monomer case. The bonded complexes follow the non-bonded complexes, with a significant difference in the BEs between the most optimal non-bonded structure, (a), and the most optimal bonded structure, (d).

Figure 8(ii) shows the dimers with two water molecules. The trends are as follows: water molecules tend to remain together and the largest BEs are associated with the non-bonded anthracene dimer with a side orientation to the water sub-clusters (structures (a), (b), and (c)). The next structures are structure (d) and (e), where the

water molecules are on separate sides of the anthracene dimer. The least stable structures are (f) and (g), where the anthracene dimer is covalently bonded. Structure (f) is more stable then (g) as in this structure the two water are clustered on the same side of the dimer while in (ii-g) the water sub-cluster is divided. (g)Figure 8 Panels (iii) and (iv) show the ionized structures with 3 and 4 water molecules, respectively. Once again, we observe that the order of stability follows the ionized anthracene dimers. The most stable structures are those with non-bonded anthracene dimers, and water tends to remain in clusters.

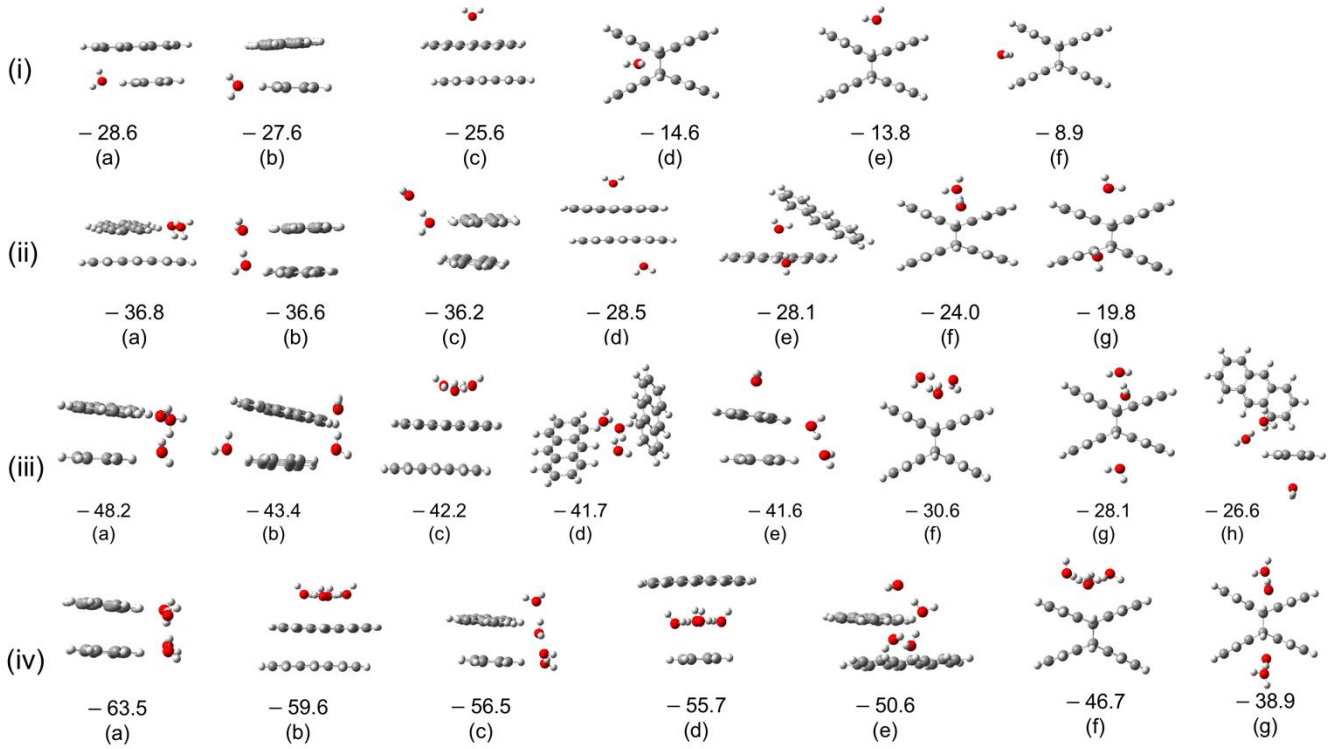

Figure 8: Ionized anthracene dimer complexed to one (i), two (ii), three (iii) and four (iv) water molecules.

Electronic States of Photoionized PAHs

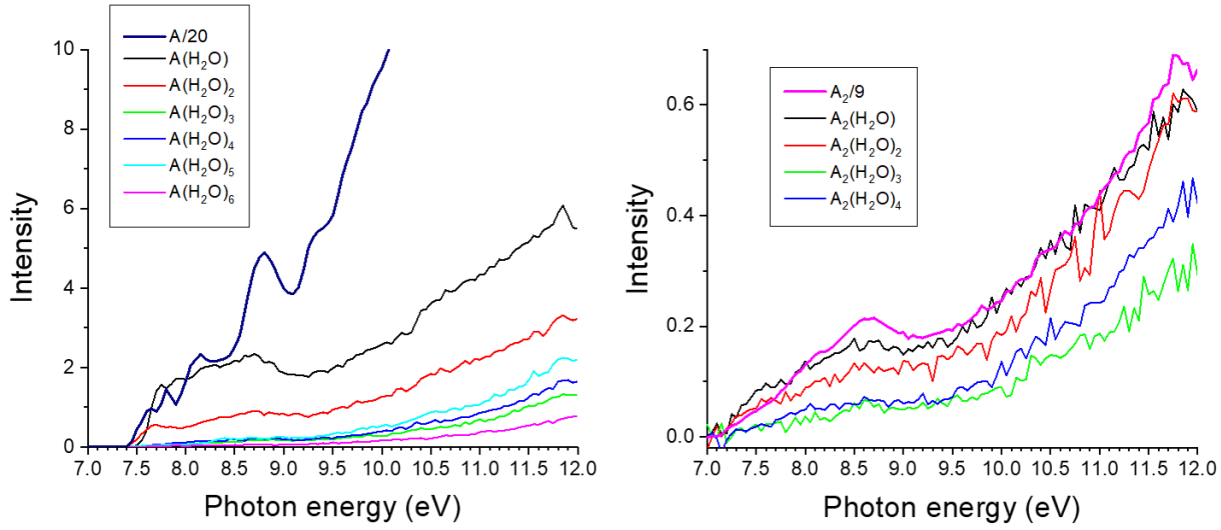

Figure 9: Photoionization efficiency curves and appearance energy determinations of anthracene-water clusters. The intensity of anthracene monomers and dimers is divided by 20 and 9, respectively, in order to display it on the same scale as that of the anthracene-water clusters.

Figure 9 A and B show the photoionization efficiency (PIE) curves for anthracene and anthracene dimers, respectively, clustered with water. While the anthracene monomer exhibits a structured curve, a less structured curve is observed in the dimer case. The anthracene monomer curve fits earlier experimental determination extremely well (see SI Figure S1). The addition of one water molecule to anthracene leads to a dramatic change in the shape, the peaks tend to shift and broaden out, and this trend continues with the addition of a second water molecule. Adding additional water molecules causes the curves to resemble each other, with no discernable structure. In Figure 9B, we see that upon dimerization, the structure also tends to smooth out, compared with the monomer, and that the addition of water leads to almost similarly shaped PIEs. The ionization energies extracted from these PIE curves, and the general change in shape upon dimerization of anthracene and clustering of water molecules are described together with the theoretical calculations later in the text. An added complication to recording PIE's is the fact that fragmentation of larger clusters is possible with the excess energy that is imparted into the cluster system beyond the ionization energy. However, we do not believe it will perturb the PIE curves dramatically. Comparing experimental results with theory, we have previously shown that PIEs can adequately reflect ionization of the parent system in the case of the water dimer[41], and thymine water clusters[42]. It is believed that the excess energy in single photon ionization at threshold tends to be released in the kinetic energy of the departing electron. [43]

Hence, insight into the ionized electronic states can be obtained from PIE curves presented in Figure 9. Additionally, from the PIEs, we can extract the IE of the structures, which are shown in Table 1.

Table 1 Experimental and calculated ionization energies (IE) of anthracene-water (A_nW_n) clusters in eV. A_2W_n-cluster nomenclature (a to f) follows the indexing utilized in Figures 3, 4 and 5.

species	**experimental**	**calculated**					
monomer	IE (eV)	A					
A	7.4	7.4					
		W_{top}	W_{side}				
AW	7.5	7.6	7.1				
AW_2	7.4	7.7	7.4				
AW_3	7.5	7.6	7.5				
AW_4	7.5	7.4	7.4				
AW_5	7.5	-	-				
AW_6	7.5	-	-				
dimer	IE (eV)	a	b	c	d		
A_2	7.1	7.8	7.2	7.0	7.2		
		a	b	c	d	e	f
A_2W	7.2	7.1	7.2	7.2	-	-	-
A_2W_2	7.2	7.1	7.0	7.0	7.3	7.5	7.3
A_2W_3	7.3	7.2	7.0	6.9	7.2	7.4	-
A_2W_4	7.3	7.0	7.2	7.1	7.0	-	-

The measured experimental IE of anthracene is 7.4 eV (Figure S1), which is in excellent agreement with the calculated value of 7.4 eV. The measured IE of the dimer is 7.1 eV, and this value is consistent with the calculated values for the non-bonded dimers, which are 7.2 eV (Figure 3, structure b) and 7.0 eV (Figure 3, structure c). We observe a decrease in the IE from the monomer to the dimer, in agreement with previous observations of a reduction in the appearance energy of naphthalene with additions of monomer units.[29] To understand the trends observed in the spectra, we calculated the possible ionized states of anthracene from different electronic levels – depending on the available energy.

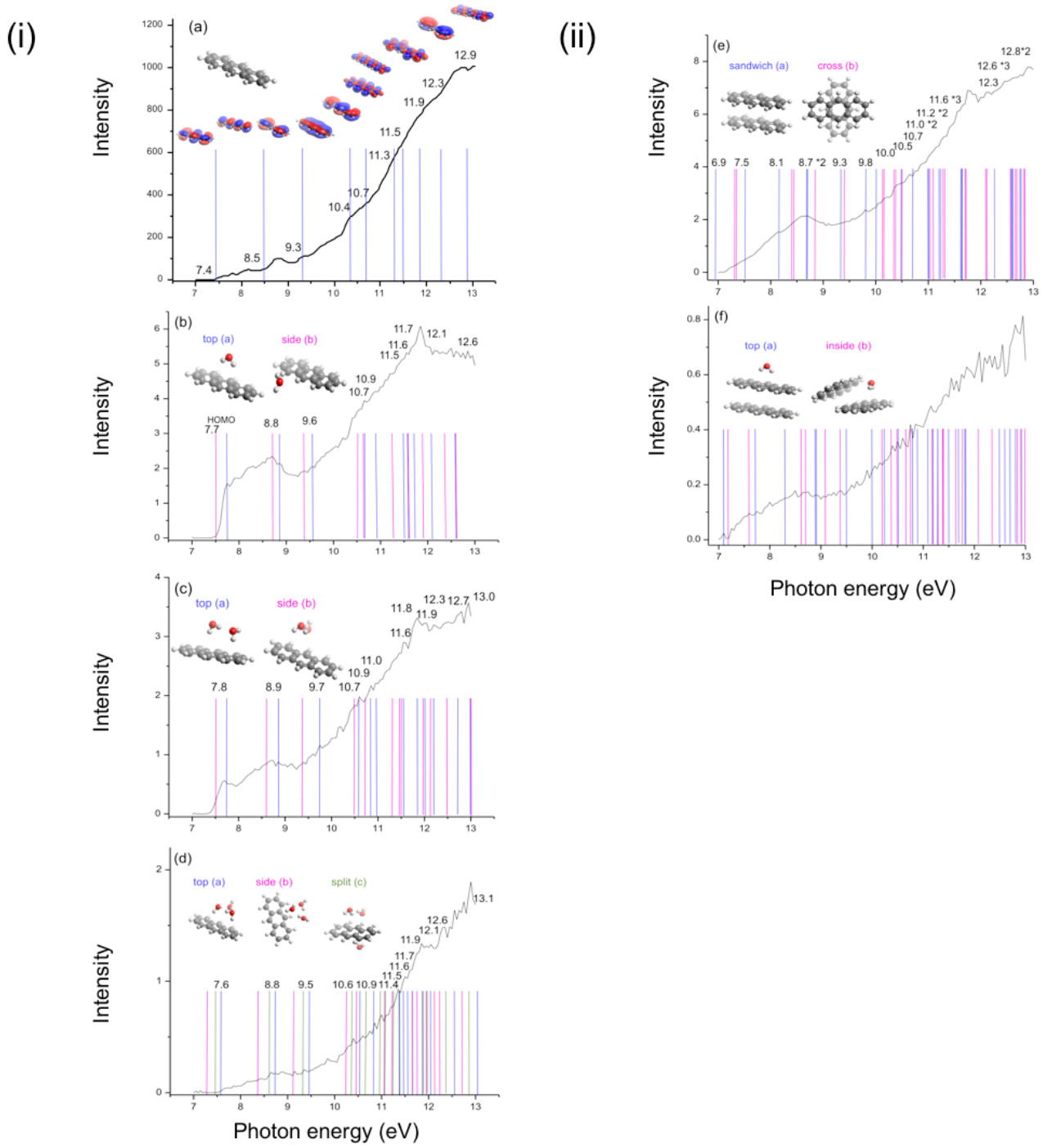

Figure 10: Ionized states calculated for different isomers corresponding to a monomer with water (i) and a dimer with water (ii): (i-a) A, $(\mathrm{i}-\mathrm{b})AW$, $(\mathrm{i}-\mathrm{c})\ AW_2$, (i-d) AW_3, (ii-e) A_2, and $(\mathrm{ii}-\mathrm{f})\ A_2\mathrm{W}_2$. Theoretical intensities are superimposed on the experimental photoionization efficiency curve and do not represent calculated intensities.

Figure 10(i-a) shows the molecular orbitals of anthracene from which electrons can be removed, with the energy corresponding to each state. Ionization is possible from states HOMO to HOMO -9 in the experimental energy

range; adding one water molecule to anthracene results in a slight shift of the energies of the ionized states, as demonstrated in Figure 10(i-b). Additionally, because more than one orientation of the water molecule with respect to the anthracene molecule is possible (specifically: side and on-top orientations), from each orientation, we observe different contributions with similar energies (in the figure, blue denotes the on-top orientation and pink denotes the side orientation). We also observe an ionized state with the water molecule (at 11.6 eV for the on-top orientation and 12.6 eV for the side orientation). The exact ionization energies are given in the SI, Table TS3. For the AW_2 system (Figure 10(i-c)), again, both the on-top and side orientations are calculated (blue and pink lines in the figure, respectively), and both exhibit similar, slightly shifted energies compared with the ionized states. In this case, several more isomers are possible, likely resulting in similar energies for each ionized state of anthracene. Moreover, more ionized states are possible for each isomer (ionization can occur from up to HOMO -11). In the case of the AW_3 system (Figure 10(i-d)), we calculated three different orientations (note that more are possible): top (blue), side (pink), and split (green). The energies of the ionized state of the different orientations are again similar. The abundance of lines along with an increased number of isomers results in the loss of structure in the PIE.

The spectrum of the anthracene dimer is presented in Figure 10(ii-e). For the dimer state, there are many more possible states than for the monomer state in the experiment's energy range. In addition, more than one isomer is possible, which gives rise to a slightly different line and thus, a less structured spectrum is expected. The abundance of lines also increases when adding water molecules due to the numerous possible orientations, each contributing to the spectra, and resulting in a complete loss of structure, as observed in the experiments.

Water confinement and the influence of ionized anthracene on the structure of 4 water clusters

An interesting result arises from the calculations, in the case of neutral A_2W_4, we observe a stable isomer in which the water cluster is confined between the two anthracene units. In a stable isolated water cluster containing four water molecules, two non-contiguous hydrogen atoms point up, and the other two point down. The confinement becomes possible only in a cross configuration of the anthracene dimer. In this configuration, the hydrogen atoms pointing up interact via OH$\cdots\pi$ with the anthracene above them, and the two hydrogen atoms pointing down interact via OH$\cdots\pi$ with the anthracene below them, as demonstrated in Figure 11.

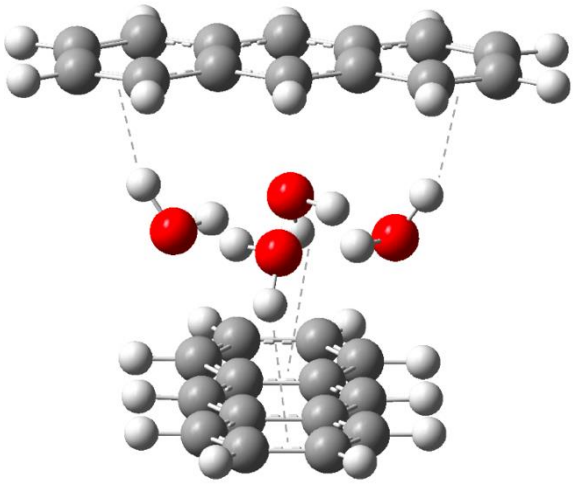

Figure 11: Four water cluster confined in anthracene dimer in a cross configuration.

In the case of a three-water cluster, two hydrogen atoms point up, and one hydrogen atom points down; thus, one

of the rings contains only one OH$\cdots\pi$. The lack of the additional OH$\cdots\pi$ interaction with one of the anthracenes results in its rotation to maximize CH$\cdots$O interaction, and the water cluster is no longer confined. These reasons explain why confinement was not observed in the case of naphthalene with a four-water cluster[24]; due to the size of the acene, the OH$\cdots\pi$ interactions are not optimal.

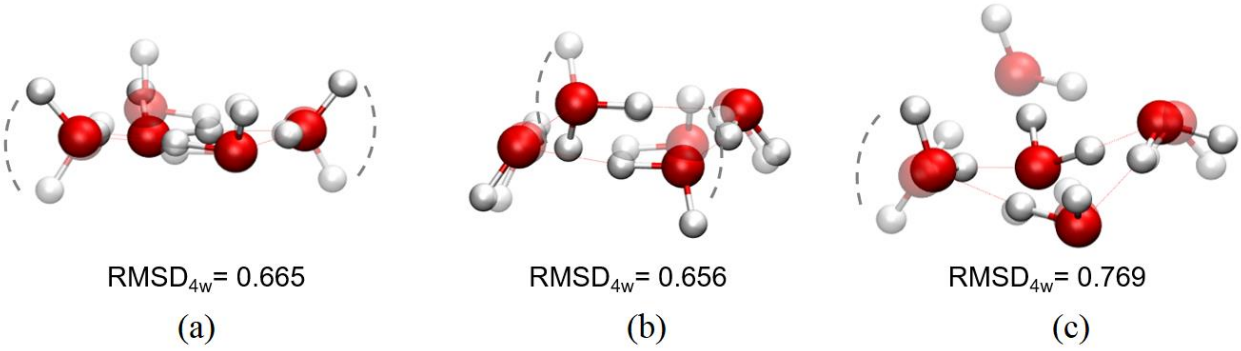

Figure 12: Difference of the water sub-clusters in Structures (iv-b), (iv-d), and (iv-f) in Figure 8 with respect to isolated water clusters. Plain atoms: configuration of the water cluster in the presence of the anthracene dimer. Transparent atoms: configuration of the isolated water cluster. For each case, the RMSD between the clusters is reported.

We demonstrated that upon ionization, the water tends to remain clustered. However, structural changes in the water are observed; the calculation of the water dimer started with the optimal structure of four isolated water cluster; thus, the observed structural changes at the end of the calculations are due to the presence of the ionized dimer. To study the effect of the ionized anthracene dimer on the water sub-cluster, we calculated the root mean square deviation (RMSD) between the different structures (namely, between the isolated (neutral) water cluster and the water sub-cluster in structures (iv-b), (iv-d), and (iv-f) in Figure 8). The RMSD compares the coordinates of the two clusters and thus gives us a measure of the structural changes that occurred. If the structures are completely identical, then the RMSD would be zero. The larger the RMSD is, the larger the differences between the structures. Figure 12 presents visually the difference between the isolated water clusters and the water clusters in the presence of the anthracene dimer taken from Structures (iv-b), (iv-d), and (iv-f) in Figure 8. The RMSD values and Figure 12 (a-c) demonstrate that there is indeed structural change in the water sub-cluster. Instead of having interleaved hydrogen atoms (one up, one down), the water cluster changes into configurations where two or more adjacent protons are pointing in the same direction (up-up or down-down). To obtain better insight into these changes, we calculated the hole due to ionization by comparing the electron density of the neutral structure and the cation with the neutral geometry (i.e., before structural relaxation). The results are presented in Figure 13.

Observing the hole in the different structures explains the structural changes in the water clusters. For example, in the unbonded anthracene structures, (a) and (b), in Figure 13, extra stabilization of the system is possible due to the oxygen atoms moving closer to the hole of the molecule and the hydrogen atoms pointing away from it. The isolated water cluster with four hydrogen atoms pointing to the same side is 3.3 kcal/mol less stable than the water cluster where adjacent water molecules have their protons pointing in opposite directions. In the case of Structure (c) in Figure 13, the hole is not in the anthracene right next to the water cluster. This results in a lack of extra stabilization from the oxygen-hole interaction, and we observe the "flipping" of only one of the protons. Thus, the water sub-cluster is in a configuration that is energetically more favorable.

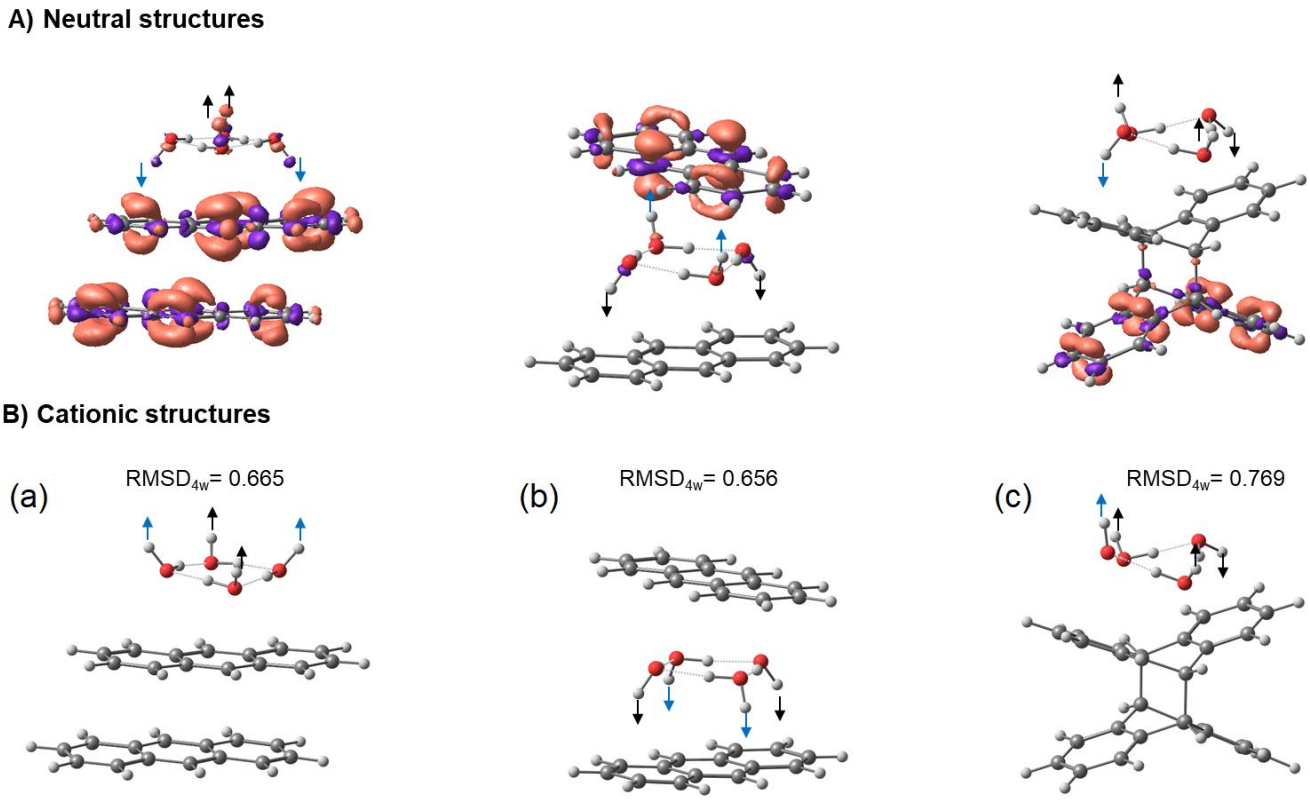

Figure 13: Electron hole due to ionization of the neutral structures (top panel) and relaxed cationic structures (bottom panel) (a): Figure 8 (iv-b), (b): Figure 8 (iv-d), and (c): Figure 8 (iv-f). Hydrogen atoms on the water molecules that preserve their orientation (up or down) with respect to the oxygen atoms in the neutral clusters are marked with a black arrow. In contrast, a blue arrow represents a "flipped" hydrogen atom when compared with the neutral structure.

Conclusion

Photoionization mass spectrometry coupled to tunable VUV radiation from a synchrotron allowed us to study the anthracene monomer and dimer and their hydration by water clusters. Experimental photoionization efficiency spectra reveal a loss of structure when shifting from the monomer to the dimer and when adding water units. This loss of structure, or smoothing, indicates the presence of several isomers in the beam. We studied the structure of these clusters using density functional theory both as neutrals and upon subsequent photoionization. In the case of the anthracene monomer with differing numbers of water molecules, the most stable isomers are those with OH$\cdots\pi$ and CH$\cdots$O interactions between the water cluster and the aromatic ring. In the case of A_2W_n, the stability trends follow that of the anthracene dimers. When comparing structures of the same dimer isomer with a different distribution of the water clusters, it is clear that the energetic tendency of the water molecules is to remain clustered. Theoretically we show that in all cases, except for four water molecules, water clusters are not confined inside the anthracene dimers, and structures with an OH$\cdots\pi$ interaction with one ring and a CH$\cdots$O interaction with the second ring are preferred. When the anthracene unit is ionized, we see hydrogen bond chain formation in the case of AW_n where n = 1,2. When n=3,4, the preference is to form a cyclic water cluster above the aromatic ring. Here, the clusters are flipped so that the oxygen is pointing toward the ionized ring. In ionized A_2W_n, the structures again follow the stability of the dimer; however, we observe a reversal in the stability trends in dimer structure: the bonded system is the least stable on the cationic surface. As one of the anthracenes is ionized, in some cases we observe more CH$\cdots$O interaction and the tendency of the water molecules to be in a side orientation to the aromatic rings. Here as well, the preference of the water is to remain clustered together and not to spread around the anthracenes. As a result of the ionization, the water cluster progresses through structural changes so that the oxygen points toward the hole and the hydrogen atoms point away from it. Theoretically, confinement of a water cluster was observed only in the case of A_2W_4.

Acknowledgements

The Israel Science Foundation funded work at the Hebrew University under Grant No. 1941/20. Work at the Advanced Light Source is supported by the Director, Office of Science, Office of Basic Energy Sciences, of the US Department of Energy under Contract No. DE-AC02-05CH11231 through the Gas Phase Chemical Physics Program, Chemical Sciences Division. This research used resources of the Advanced Light Source, a Department of Energy (DOE) Office of Science User Facility under the same contract.

1. Meyer, E.A., R.K. Castellano, and F. Diederich, *Interactions with Aromatic Rings in Chemical and Biological Recognition.* Angewandte Chemie International Edition, 2003. **42**(11): p. 1210-1250.
2. McKenzie, S. and H.C. Kang, *Squeezing water clusters between graphene sheets: energetics, structure, and intermolecular interactions.* Physical Chemistry Chemical Physics, 2014. **16**(47): p. 26004-26015.
3. Holt, J.K., et al., *Fast Mass Transport Through Sub-2-Nanometer Carbon Nanotubes.* Science, 2006. **312**(5776): p. 1034-1037.
4. Radha, B., et al., *Molecular transport through capillaries made with atomic-scale precision.* Nature, 2016. **538**(7624): p. 222-225.
5. Song, W., et al., *Artificial water channels enable fast and selective water permeation through water-wire networks.* Nature Nanotechnology, 2020. **15**(1): p. 73-79.
6. Majumder, M., et al., *Enhanced flow in carbon nanotubes.* Nature, 2005. **438**(7064): p. 44-44.
7. Dopfer, O. and M. Fujii, *Probing Solvation Dynamics around Aromatic and Biological Molecules at the Single-Molecular Level.* Chemical Reviews, 2016. **116**(9): p. 5432-5463.
8. Salonen, L.M., M. Ellermann, and F. Diederich, *Aromatic Rings in Chemical and Biological Recognition: Energetics and Structures.* Angewandte Chemie International Edition, 2011. **50**(21): p. 4808-4842.
9. Öberg, K.I., *Photochemistry and Astrochemistry: Photochemical Pathways to Interstellar Complex Organic Molecules.* Chemical Reviews, 2016. **116**(17): p. 9631-9663.
10. Cuylle, S.H., L.J. Allamandola, and H. Linnartz, *Photochemistry of PAHs in cosmic water ice.* A&A, 2014. **562**: p. A22.
11. Michoulier, E., et al., *Theoretical determination of adsorption and ionisation energies of polycyclic aromatic hydrocarbons on water ice.* Physical Chemistry Chemical Physics, 2018. **20**(17): p. 11941-11953.
12. Pérez, C., et al., *Corannulene and its complex with water: a tiny cup of water.* Physical Chemistry Chemical Physics, 2017. **19**(22): p. 14214-14223.
13. Domingos, S.R., et al., *Water Docking Bias in [4]Helicene.* Angewandte Chemie International Edition, 2019. **58**(33): p. 11257-11261.
14. Loru, D., et al., *How does the composition of a PAH influence its microsolvation? A rotational spectroscopy study of the phenanthrene–water and phenanthridine–water clusters.* Physical Chemistry Chemical Physics, 2021. **23**(16): p. 9721-9732.
15. Chatterjee, K., et al., *Unravelling the microhydration frameworks of prototype PAH by infrared spectroscopy: naphthalene–(water)1–3.* Physical Chemistry Chemical Physics, 2021. **23**(25): p. 14016-14026.
16. Attah, I.K., et al., *Hydrogen bonding of the naphthalene radical cation to water and methanol and attachment of the naphthalene ion to extended hydrogen bonding chains.* Chemical Physics Letters, 2014. **613**: p. 45-53.
17. Alata, I., et al., *Microhydration effects on the electronic spectra of protonated polycyclic aromatic hydrocarbons: [naphthalene-(H2O)n = 1,2]H+.* The Journal of Chemical Physics, 2011. **134**(7): p. 074307.
18. Palmer, P.M. and M.R. Topp, *Electronic spectroscopy of jet-cooled anthracene/(H2O)n clusters (n=1–16): comparisons of inhomogeneous structure.* Chemical Physics, 1998. **239**(1): p. 65-81.
19. Le Page, V., et al., *Reactions of Cations Derived from Naphthalene with Molecules and Atoms of Interstellar Interest.* Journal of the American Chemical Society, 1999. **121**(40): p. 9435-9446.
20. Chatterjee, K. and O. Dopfer, *Microhydration of PAH+ cations: evolution of hydration network in naphthalene+-(H2O)n clusters (n ≤ 5).* Chemical Science, 2018. **9**(8): p. 2301-2318.
21. Lietard, A., G. Mensa-Bonsu, and J.R.R. Verlet, *The effect of solvation on electron capture revealed using anion two-dimensional photoelectron spectroscopy.* Nature Chemistry, 2021. **13**(8): p. 737-742.
22. Sharma, D. and M.J. Paterson, *Ground and excited states of naphthalene–water (naphtha–W6) clusters: a computational study.* RSC Advances, 2015. **5**(36): p. 28281-28291.
23. Hernández-Rojas, J., et al., *Modeling Water Clusters on Cationic Carbonaceous Seeds.* The Journal of Physical Chemistry A, 2010. **114**(27): p. 7267-7274.

24. Hirunsit, P. and P.B. Balbuena, *Effects of Confinement on Small Water Clusters Structure and Proton Transport.* The Journal of Physical Chemistry A, 2007. **111**(42): p. 10722-10731.
25. Cabaleiro-Lago, E.M., J. Rodríguez-Otero, and Á. Peña-Gallego, *Computational Study on the Characteristics of the Interaction in Naphthalene···(H2X)n=1,2 (X = O, S) Clusters.* The Journal of Physical Chemistry A, 2008. **112**(28): p. 6344-6350.
26. Takeuchi, H., *Structures, stability, and growth sequence patterns of small homoclusters of naphthalene, anthracene, phenanthrene, phenalene, naphthacene, and pyrene.* Computational and Theoretical Chemistry, 2013. **1021**: p. 84-90.
27. Grimme, S., C. Diedrich, and M. Korth, *The Importance of Inter- and Intramolecular van der Waals Interactions in Organic Reactions: the Dimerization of Anthracene Revisited.* Angewandte Chemie International Edition, 2006. **45**(4): p. 625-629.
28. Zade, S.S., et al., *Products and Mechanism of Acene Dimerization. A Computational Study.* Journal of the American Chemical Society, 2011. **133**(28): p. 10803-10816.
29. Xu, B., et al., *Probing solvation and reactivity in ionized polycyclic aromatic hydrocarbon–water clusters with photoionization mass spectrometry and electronic structure calculations.* Faraday Discussions, 2019. **217**(0): p. 414-433.
30. Shao, Y., et al., *Advances in molecular quantum chemistry contained in the Q-Chem 4 program package.* Molecular Physics, 2015. **113**(2): p. 184-215.
31. Mardirossian, N. and M. Head-Gordon, *[small omega]B97X-V: A 10-parameter, range-separated hybrid, generalized gradient approximation density functional with nonlocal correlation, designed by a survival-of-the-fittest strategy.* Physical Chemistry Chemical Physics, 2014. **16**(21): p. 9904-9924.
32. Dunning , T.H., Jr, *Gaussian basis sets for use in correlated molecular calculations. I. The atoms boron through neon and hydrogen.* The Journal of Chemical Physics, 1989. **90**(2): p. 1007-1023.
33. Krylov, A.I., *Equation-of-Motion Coupled-Cluster Methods for Open-Shell and Electronically Excited Species: The Hitchhiker's Guide to Fock Space.* Annual Review of Physical Chemistry, 2008. **59**(1): p. 433-462.
34. Pieniazek, P.A., et al., *Benchmark full configuration interaction and equation-of-motion coupled-cluster model with single and double substitutions for ionized systems results for prototypical charge transfer systems: Noncovalent ionized dimers.* The Journal of Chemical Physics, 2007. **127**(16): p. 164110.
35. Khistyaev, K., et al., *Proton Transfer in Nucleobases is Mediated by Water.* The Journal of Physical Chemistry A, 2013. **117**(31): p. 6789-6797.
36. Weigend, F., A. Köhn, and C. Hättig, *Efficient use of the correlation consistent basis sets in resolution of the identity MP2 calculations.* The Journal of Chemical Physics, 2002. **116**(8): p. 3175-3183.
37. Lu, W., et al., *Exciton energy transfer reveals spectral signatures of excited states in clusters.* Physical Chemistry Chemical Physics, 2020. **22**(25): p. 14284-14292.
38. Golan, A. and M. Ahmed, *Ionization of Water Clusters Mediated by Exciton Energy Transfer from Argon Clusters.* The Journal of Physical Chemistry Letters, 2012. **3**(4): p. 458-462.
39. Gregory, J.K., et al., *The Water Dipole Moment in Water Clusters.* Science, 1997. **275**(5301): p. 814-817.
40. Steber, A.L., et al., *Capturing the Elusive Water Trimer from the Stepwise Growth of Water on the Surface of the Polycyclic Aromatic Hydrocarbon Acenaphthene.* The Journal of Physical Chemistry Letters, 2017. **8**(23): p. 5744-5750.
41. Kamarchik, E., et al., *Spectroscopic signatures of proton transfer dynamics in the water dimer cation.* The Journal of Chemical Physics, 2010. **132**(19): p. 194311.
42. Khistyaev, K., et al., *The effect of microhydration on ionization energies of thymine.* Faraday Discussions, 2011. **150**(0): p. 313-330.
43. Dong, F., et al., *Dynamics and fragmentation of van der Waals clusters: (H2O)n, (CH3OH)n, and (NH3)n upon ionization by a 26.5eV soft x-ray laser.* The Journal of Chemical Physics, 2006. **124**(22): p. 224319.